A COLE-COLE DIAGRAM REPRESENTATION OF MICROSTRIP STRUCTURE

S. Malisuwan
Department of Electrical Engineering
Chulachomklao Royal Military Academy
Nakhon-Nayok, Thailand

P.S. Neelakanta and V. Ungvichian
Department of Electrical Engineering
Florida Atlantic University
Boca Raton, FL 33432, USA.

Abatract—A method for analyzing the performance of a microstrip line using the concept of Cole-Cole diagram, is proposed. Analogous to dielectric relaxation considerations of Cole-Cole diagrams as applied to dielectric materials, a "reactive relaxation" concept is introduced to represent the frequency-dependent characteristics of a microstrip. Also, included in the algorithm are relevant considerations pertinent to the substrate dielectric and strip-line conductor losses. The dynamic permittivity of the microstrip structure (deduced via Cole-Cole diagram) leads to a convenient and modified Smith-chart representation that includes the frequency-dependent influence of the fringing field and the lossy characteristics of the line cohesively. The efficacy of the model is illustrated with an example concerning a microstrip patch antenna in ISM band. Relevant algorithms are useful in computer-aided designs (CADs).

Indexing Terms—Cole-Cole diagram, Microstrip structure, Microstrip patch antenna, Modified Smith chart, CAD.

1. INTRODUCTION

The microstrip line is one of the most popular types of planar transmission lines, primarily because it is easily integrated with other passive and active microwave devices. Relevant design equations in closed-form using semi-empirical strategies specifying the frequency-dependent, effective dielectric permittivity concept and dispersion characteristics of a microstrip line have been derived in the existing literature [1]-[7]. Although many computer-aided design (CAD) systems have been developed using such algorithms with built-in microstrip design capabilities, simple calculation methods for microstrip line parameters by hand-calculator and/or by personal computer are needed for preliminary design purposes, and/or for quick circuit evaluation purposes. Moreover, designers may need to observe the physical considerations of microstrip circuits on step-by-step basis. Therefore, many researchers are in search of simple methods, which are at the same time and sufficient to explain the physical aspects of microstrip circuits, precisely.

In this research an approach that uses the Debye relation [8] is introduced to develop an "equivalent relaxation diagram" (analogous to the Cole-Cole diagram) that represents the frequency-dependent, lossy and lossless capacitive characteristics of a microstrip line structure. Further, the frequency-dependent, lossy characteristics of microstrip lines are addressed via Smith chart representation. Results based on the proposed model are compared with the available data in the literature in respect of a microstrip patch antenna.

2. MICROSTRIP-BASED EQUIVALENT RELAXATION PROCESS

The Debye relation on the relative complex permittivity of a material depicting the dielectric relaxation can be written as [9]:

$$\varepsilon_m^*(\omega) = \varepsilon_\infty + \frac{\varepsilon_s - \varepsilon_\infty}{1 + j2\pi(\omega/\omega_r)} \tag{1a}$$

$$\text{or } \varepsilon_m^*(\omega) = \left[\varepsilon_\infty + \frac{\varepsilon_s - \varepsilon_\infty}{1+4\pi^2(\omega/\omega_r)^2}\right] - j\left[(\varepsilon_s - \varepsilon_\infty)\frac{2\pi(\omega/\omega_r)}{1+4\pi^2(\omega/\omega_r)^2}\right] \tag{1b}$$

where $\omega = 2\pi f$; f is the applied frequency; and, $f_r = 1/\tau_r$ where τ_r is the characteristic relaxation time of the dielectric material. Further, ε_∞ and ε_s are the relative permittivities of the material at very high ($f \to \infty$) and quasi-static ($f \to 0$) frequencies.

The concept of dielectric relaxation can be analogously applied to characterize the frequency-dependent performance of a microstrip line. Hence, Kirschning and Jansen' frequency-dependent effective permittivity deduced for a microstrip [5] can be written in a Debye relation form as follows:

$$\varepsilon_u'(\omega) = \varepsilon_{eff}(\omega) = \left[\varepsilon_r + \frac{\varepsilon_{eff}(0,u) - \varepsilon_r}{1+Q(\omega,u)}\right] \equiv \text{Re}\left[\varepsilon_r + \frac{\varepsilon_{eff}(0,u) - \varepsilon_r}{1 + j(1/2\pi)(\omega_o/\omega)}\right] \tag{2}$$

where u is the line-width to substrate-thickness ratio, $(w/\lambda)/(h/\lambda)$; ε_r is the dielectric constant of the substrate; $\varepsilon_{eff}(0, u)$ is the equivalent (relative) static permittivity; and $Q(\omega, u)$ is a dimension-dependent factor [5] and λ is the wavelength of operation.

The frequency-dependent effective permittivity in Eqn. (2), it can be equated to the real part of Eqn. (1b) as follows.

$$\varepsilon_r + \frac{\varepsilon_{eff}(0,u) - \varepsilon_r}{1 + Q(\omega,u)} = \varepsilon_\infty + \frac{\varepsilon_s - \varepsilon_\infty}{1 + 4\pi^2(\omega/\omega_r)^2} \tag{3}$$

This gives,

$$\varepsilon_r = \varepsilon_\infty \tag{4}$$

$$\varepsilon_{eff}(0,u) = \varepsilon_s \tag{5}$$

$$\tau_o = \frac{\sqrt{Q(\omega,u)}}{\omega} \tag{6}$$

Now, an "imaginary part" of the equivalent permittivity of a microstrip system can be obtained by applying Eqns. (4)-(6) into the imaginary part of Eqn. (1b). Hence, the imaginary part of Cole-Cole expression for a microstrip system can be written as

$$\varepsilon_u''(\omega) = \left[\frac{(\varepsilon_{eff}(0,u) - \varepsilon_r)\sqrt{Q(\omega)}}{1+Q(\omega)}\right] \tag{7}$$

Hence, the complex permittivity of microstrip system in compact form can be written as:

$$\varepsilon_u^*(\omega) = \varepsilon_r + \frac{\varepsilon_{eff}(0) - \varepsilon_r}{1 + j(1/2\pi)(\omega_o/\omega)} \tag{8}$$

By illustrating the relevant Debye relations via Cole-Cole diagrams, a lateral inversion as shown in Eqns. (1a) and (8) can be noticed. That is, the material-based and microstrip-based Cole-Cole diagrams are laterally inverted in a mirror-image fashion as shown in Figs. 1 and 2.

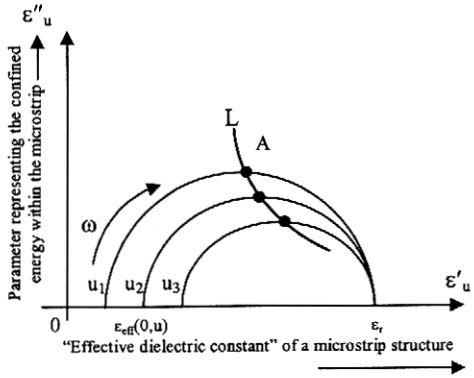

Fig. 1 Cole-Cole representation of reactive relaxation of a microstrip structure with u = (w/λ)/(h/λ) and u1 < u2 < u3

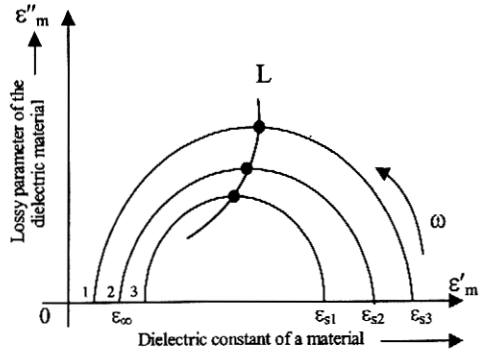

Fig. 2 Cole-Cole diagram of Debye relaxation in a dielectric material with $\varepsilon_{s1} < \varepsilon_{s2} < \varepsilon_{s3}$ and $\tau_r(\varepsilon_{s1}) < \tau_r(\varepsilon_{s2}) < \tau_r(\varepsilon_{s3})$

Further, the maximum points of semi-circles in the Cole-Cole patterns correspond to maximum Debye loss in a lossy dielectric material; but, in respect of a microstrip system, these points can be regarded as to depict the maximum reactive (capacitive) energy confined within the microstrip structure. That is, pertinent to these maximum value points (A) in Fig. 1, it can be considered that the microstrip geometry holds the field within itself, rather letting it to fringe out. In material-based diagram (Fig. 2), it can be observed that loss in the material increases with dielectric constant. In contrast, in the microstrip-based diagram (Fig. 1), there is a reduction in the extent of energy confined when u = (w/λ)/(h/λ) ratio is increased. That is because, an increase in fringing field results in with decreasing substrate thickness.

Considering the equivalent Cole-Cole diagram of the test microstrip depicted in Fig. 3, the simulation results reveal that the nonfringing part of the reactive energy in the microstrip reduces when the (w/λ)/(h/λ) ratio increases. For example, about 10% reduction of this nonfringing energy is observed when the (w/λ)/(h/λ) ratio is increased from 1.0 to 2.0 for both dielectric materials. The results also indicate that the extent of the energy confined within microstrip line without proliferation as fringe fields increases with the dielectric constant of the substrate.

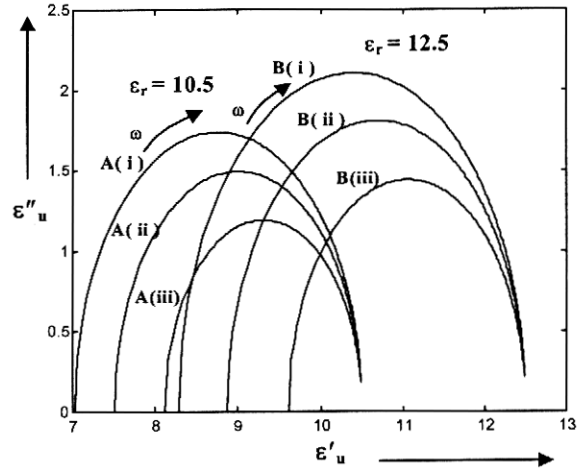

Fig. 3 Cole-Cole diagram for the test microstrip structures
curves A: alumina ($\varepsilon_r = 10.5$)
curves B: gallium arsenide ($\varepsilon_r = 12.5$)
(i) (w/λ)/(h/λ)= 1.0 (ii) (w/λ)/(h/λ) = 2.0
(iii) (w/λ)/(h/λ) = 4.0

The equivalent Cole-Cole diagram for the microstrip line (Fig. 1) can be further modified to include the lossy attributions. That is, in the event that the stripline has a lossy substrate and/or when the metallic strip poses a conduction loss, the relevant considerations can be appropriately included in the Cole-Cole representation of Fig. 1.

The conductor loss of the strip can be added as a lossy component into the imaginary part of the equivalent permittivity of the microstrip system. Considering the attenuation (in Np/m) due to the transmission along a microstrip conductor as specified in [3]:

$$\alpha_c \cong \sqrt{\pi f \mu_o \sigma_{eff}} \equiv \frac{\sqrt{\varepsilon_{eff}(0,u)}\exp\left[-1.2(Z_0(0)/\eta_o)^{0.7}\right]\sqrt{\pi f \mu_o}}{Z_0(0) w \sqrt{\sigma_c}} \tag{9}$$

where σ_{eff} represents the effective loss constituent of the microstrip conductor and $Z_0(0)$ is the quasi-static characteristic impedance of the microstrip line in a homogeneous medium. Further, w is the line-width; σ_c is the conductivity of the microstrip line; η_o is the intrinsic impedance of free-space (377 Ω); and μ_o is the permeability of free-space ($4\pi\times10^{-7}$ H/m).

This conductor-loss can be added as a lossy component into the imaginary part of the equivalent complex permittivity of the microstrip system. The attenuation (in Np/m) due to the transmission along the microstrip conductor can be specified as:

$$\alpha_c \cong \sqrt{\pi f \mu_o \sigma_{c,eff}} \tag{10}$$

where $\sigma_{c,eff}$ represents the effective loss constituent of the microstrip conductor. Equating Eqns. (9) and (10), this

effective conductivity ($\sigma_{c,eff}$) of the microstrip can be deduced as:

$$\sigma_{c,eff} = \frac{\varepsilon_{eff}(0,u)\exp\left[-2.4(Z_0(0)/\eta_o)^{0.7}\right]}{Z_0^2(0)w^2\sigma_c} \quad (11)$$

In corporating Eqn. (11) in the Cole-Cole expression, an imaginary part of the effective permittivity of the microstrip ($-j\varepsilon''_c(\omega)$) can be written as:

$$-j\varepsilon_c''(\omega) = -j\frac{\varepsilon_{eff}(0,u)\exp\left[-2.4(Z_0(0)/\eta_o)^{0.7}\right]}{\omega\varepsilon_o\varepsilon'_u(\omega)Z_0^2(0)w^2\sigma_c} \quad (12)$$

Lastly, the substrate loss ($-j\varepsilon''_d(\omega)$) can be specified as $-j\varepsilon''_d(\omega) = -j\sigma_d/\omega\varepsilon_o\varepsilon_r$ where σ_d is the conductivity of the lossy substrate. Hence, the resultant equivalent Cole-Cole diagram representation of the microstrip system can be written as,

$$\varepsilon^*(\omega) = \varepsilon'_u(\omega) - j\varepsilon''_u(\omega) - j\varepsilon''_c(\omega) - j\varepsilon''_d(\omega) \quad (13)$$

Considering the equivalent Cole-Cole diagram of the test microstrip depicted in Fig. 4, the simulation results reveal that the nonfringing part of the reactive energy in the microstrip reduces as the $(w/\lambda)/(h/\lambda)$ ratio increases. For example, about 8% reduction of this nonfringing energy is observed when the $(w/\lambda)/(h/\lambda)$ ratio is increased from 0.5 to 1.0 for both dielectric substrate materials considered. As expected, the results also indicate that the extent of the energy confined within microstrip line (without proliferating as fringe fields) increases with the dielectric constant of the substrate; and, the reduction of energy can be observed when the substrate and conductor losses are included in the calculation.

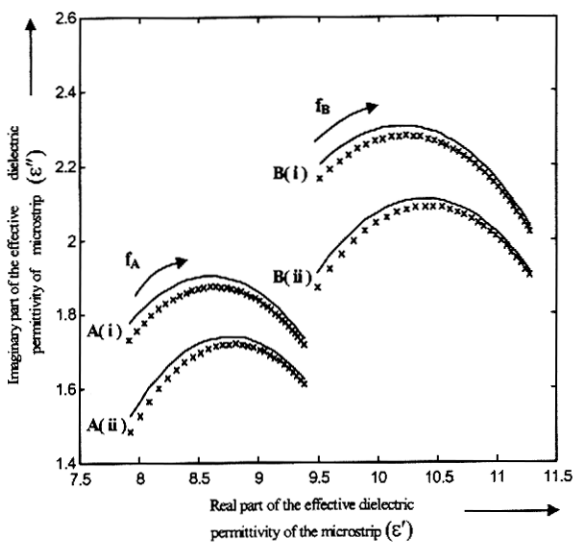

Fig. 4 Cole-Cole diagrams of test microstrip structures
$\sigma_d = 0.5$ S/m
Curves A: Alumina ($\varepsilon_r = 10.5$)
Curves B: Gallium arsenide ($\varepsilon_r = 12.5$)
(i) $u = (w/\lambda)/(h/\lambda) = 0.5$; (ii) $u = (w/\lambda)/(h/\lambda) = 1.0$
f_A: 20-60 GHz and f_B: 20-80 GHz
—— Lossless
×××× Lossy

3. FREQUENCY-DEPENDENT (LOSSY) MICROSTRIP LINE PERFORMANCE: COLE-COLE DIAGRAM BASED SMITH-CHART REPRESENTATION

The Smith-chart is an impedance representation in a complex plane depicting a set of circles of constant resistance and partial circles of constant reactance. The standard Smith-chart is based on the static characteristic impedance (Z_0) and does not include the frequency-dependent aspects of Z_0. However, it can be modified to include lossy (frequency-dependent) considerations. In this section, the concept of microstrip-based Cole-Cole diagram (developed in the last section) is applied to construct a frequency-dependent (lossy) Smith-chart to analyze microstrip line characteristics.

Before deriving the frequency-dependent Smith-chart relations, the capacitance parameter in microstrip-line system can be considered. The classical paralell-plate capacitor is shown in Fig. 5. From the geometry shown in Fig. 5, the capacitance per unit length of the structure can be expressed as [10]:

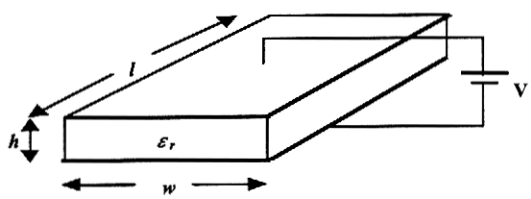

Fig. 5 A parallel-plate capacitor

$$C = \varepsilon\frac{w}{h} \quad (14)$$

A simple frequency-dependent capacitance of the parallel-plate capacitor can be modeled in terms of any frequency-dependent attributes of ε. That is,

$$C(\omega) = \varepsilon_o\varepsilon^*(\omega)\frac{w}{h} \quad (15)$$

where $\varepsilon^*(\omega)$ is a complex permittivity equal to $\varepsilon'(\omega) - j\varepsilon''(\omega)$.

Therefore,

$$C(\omega) = \varepsilon_o\varepsilon'(\omega)\frac{w}{h} - j\varepsilon_o\varepsilon''(\omega)\frac{w}{h} \quad (16)$$

Referring to the equivalent Cole-Cole diagram deduced for a parallel-plate microstrip line in Eqn. (13) is substituted into Eqn. (16). Hence,

$$C(\omega) = C\left(\frac{1}{1+Q(\omega)}\left[Q(\omega) + \frac{\varepsilon_{eff}(0)}{\varepsilon_r}\right]\right) - j\frac{C}{\varepsilon_r}\left[\varepsilon''_u(\omega) + \varepsilon''_c(\omega) + \varepsilon''_d(\omega)\right] \quad (17)$$

where $C = \varepsilon_o\varepsilon_r(w/h)$.

For simplicity, the coefficients of Eqn. (17) are defined as follows:

$$A(\omega) = \frac{1}{1+Q(\omega)}\left[Q(\omega) + \frac{\varepsilon_{eff}(0)}{\varepsilon_r}\right] \quad (18)$$

$$B(\omega) = \frac{1}{\varepsilon_r}\left[\varepsilon''_u(\omega) + \varepsilon''_c(\omega) + \varepsilon''_d(\omega)\right] \quad (19)$$

In general, the characteristic impedance of a transmission line is given by

$$Z_0 = \sqrt{\frac{R + j\omega L}{G + j\omega C}} \tag{20}$$

where R, L, G, C are per unit length quantities defined as follows:

R = resistance per unit length in Ω/m.
L = inductance per unit length in H/m.
G = conductance per unit length in S/m.
C = capacitance per unit length in F/m.

If G and C are neglected, the characteristic impedance can be written as:

$$Z_0 = \sqrt{\frac{L}{C}} \tag{21}$$

To obtain the frequency-dependent characteristic impedance ($Z_0'(\omega)$), the frequency-dependent capacitance ($C(\omega)$) of Eqn. (17) is substituted into the capacitance (C) in Eqn. (21). The resulting frequency-dependent characteristic impedance is then given by:

$$Z_0'(\omega) = \sqrt{\frac{L}{C[A(\omega) - jB(\omega)]}} = \frac{Z_0}{\sqrt{A(\omega) - jB(\omega)}} \tag{22}$$

Now, the frequency-dependent (lossy) Smith-chart can be constructed by applying $Z_0'(\omega)$ in Eqn. (22) into the normalized terminal impedance expression following the procedure as that for a standard Smith-chart [11]. Hence, the resulting normalized terminal impedance z'_L is given by

$$z'_L = \frac{Z_L}{Z_0'(\omega)} = br + jbx \qquad \text{(Dimensionless)} \tag{23}$$

where r and x are the normalized resistance and normalized reactance, respectively, and $b = \sqrt{A(\omega) - jB(\omega)}$.

Corresponding, the voltage reflection coefficient of present Smith chart can be expressed as:

$$\Gamma' = \Gamma'_r + j\Gamma'_i = \frac{z'_L - 1}{z'_L + 1} \tag{24}$$

or

$$z'_L = \frac{Z_L}{Z_0'(\omega)} = br + jbx = \frac{(1 + \Gamma'_r) + j\Gamma'_i}{(1 - \Gamma'_r) - j\Gamma'_i} \tag{25}$$

Now, the desired set of equations depicting the modified Smith-chart are:

$$\left(\Gamma'_r - \frac{br}{1 + br}\right)^2 + \Gamma_i'^2 = \frac{1}{(1 + br)^2} \tag{26}$$

and

$$(\Gamma'_r - 1)^2 + \left(\Gamma'_i - \frac{1}{bx}\right)^2 = \left(\frac{1}{bx}\right)^2 \tag{27}$$

To illustrate the construction of the proposed frequency-dependent Smith-chart, a lossy microstrip structure is considered. It consists of a gallium arsenide substrate (ε_r = 12.5) with a 1.0 mm substrate-thickness (h), 0.75 mm line-width (w) and design parameter (l/λ)/(h/λ) = 10.0. The proposed Smith-chart simulated is compared with a standard Smith-chart in Fig. 6. It can be seen that when the lossy characteristics (substrate loss, conductor loss, and frequency-dependent characteristic impedance of the microstrip line) are included in the calculation, the Smith-chart takes the form of a spiral. As well known in lossy transmission line theory that, when attenuation as a function of line-length is plotted on the Smith chart, it also takes the form of a spiral.

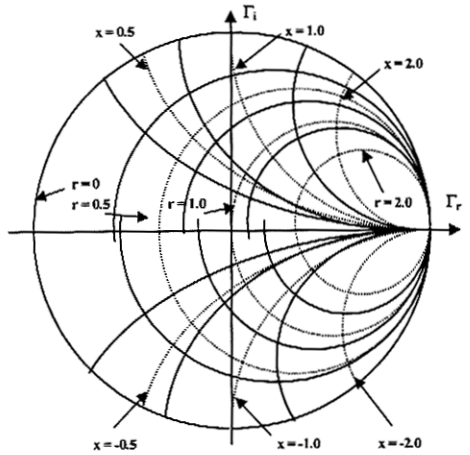

Fig. 6 The frequency-dependent (lossy) Smith chart with ε_r = 12.5; h = 1 mm, w = 0.75 mm, σ_d = 0.05 S/m, (l/λ)/(h/λ) = 10.0
——— Proposed Smith chart
..... Standard Smith chart

4. APPLICATION OF THE FREQUENCY-DEPENDENT SMITH-CHART CONSTRUCTED ON THE BASIS OF COLE-COLE DIAGRAM

This chapter is devoted to illustrate the use of frequency-dependent Smith-chart considerations deduced (on the basis of Cole-Cole diagram principle) in characterizing microstrip lines. A microstrip patch antenna is considered as a test structure for analysis.

A rectangular microstrip antenna shown in Fig. 7 is considered presently to study the frequency-dependent Smith-chart application deduced in the last section. The rectangular patch antenna in Fig. 7(a) is fed from a microstrip transmission line.

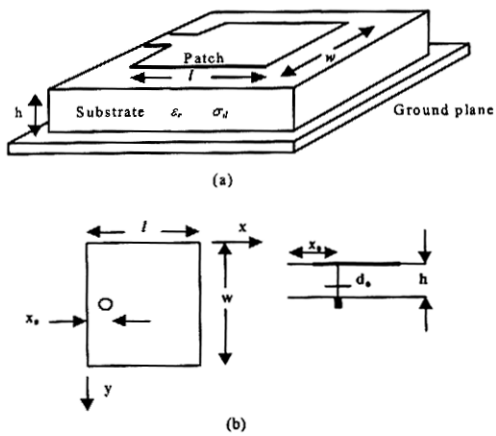

Fig. 7 Rectangular microstrip patch antenna
(a) Direct feed
(b) Coax-feed

A microstrip antenna may be excited or 'fed' by different types of transmission lines, for example coaxial (Fig. 7(b)), microstrip, or coplanar. The radiating elements may be fed directly, with electrical continuity between the conductor of the transmission line and the conducting patch. On the other hand, the microstrip patch antenna fed by a transmission line behaves as a complex impedance $Z_{in} = (R + jX)$, which depends mainly on the geometry of the coupling between the transmission line and the antenna. For direct feed (Fig. 6.1(a)), the input impedance depends strongly on the point of contact with the patch. The input impedance expressions of the microstrip patch antenna used are from Abboud's model [12].

The input impedance of the structure shown in Fig. 6.1 is given by [12]

$$Z(f) = \frac{R}{1+Q_T^2[f/f_R - f_R/f]^2} + j\left[X_L - \frac{RQ_T[f/f_R - f_R/f]}{1+Q_T^2[f/f_R - f_R/f]^2}\right] \quad (28)$$

where R is the resonant resistance including the influence of the fringing field at the edges of the patch; Q_T is the quality factor associated with system losses; f is the operating frequency; and f_R is the resonant frequency. It can be written as [12]:

$$R = \frac{Q_T h}{\pi f_R \varepsilon_{dyn} \varepsilon_o l w} \cos^2\left(\frac{\pi x_o}{l}\right) \quad (29)$$

where ε_{dyn} is the dynamic permittivity.

To take the effect of coax-feed probe (Fig. 7(b)) into account, it is necessary to modify the input impedance by an inductive reactance term [13], given by

$$X_L = \frac{377}{c_o} \ln\left(\frac{c_o}{\pi f d_o \sqrt{\varepsilon_r}}\right) \quad (30)$$

where c_o is the velocity of light in vacuum and d_o is the diameter of the probe.The detail in Eqn. (28) can be found in [12].

The flowchart of the method to calculate the input impedance of the rectangular microstrip antenna by utilizing the proposed model is shown in Fig. 8.

Fig. 9 shows the input impedance for a patch antenna operating at about 2.22 GHz. The proposed model results are compared with the computed results in [12] and measured data of [14]. The results indicate that the proposed model gives results close to the experimental data. It can also be observed that the present results are better than those predicted in [12] especially at the higher frequency range. Also, at 2.22 GHz, the result from the proposed model is closer to the measured result [12] than that calculated by [12]. The reason is that, in the proposed model, the frequency-dependent characteristic impedance is more comprehensively addressed included in the algorithm so that possible errors in the high frequency are reduced.

5. AN ANTENNA SYSTEM IN WIRELESS COMMUNICATION APPLICATIONS (2.45 GHz ISM BAND): DESIGN CONSIDERATIONS

The Industrial, Scientific and Medical (ISM) frequency bands governed by Federal Communications Commission (FCC) Part 15 specifications have seen dramatic growth in recent years, particularly the 2.4000 to 2.4835 GHz (ISM-2400) band.

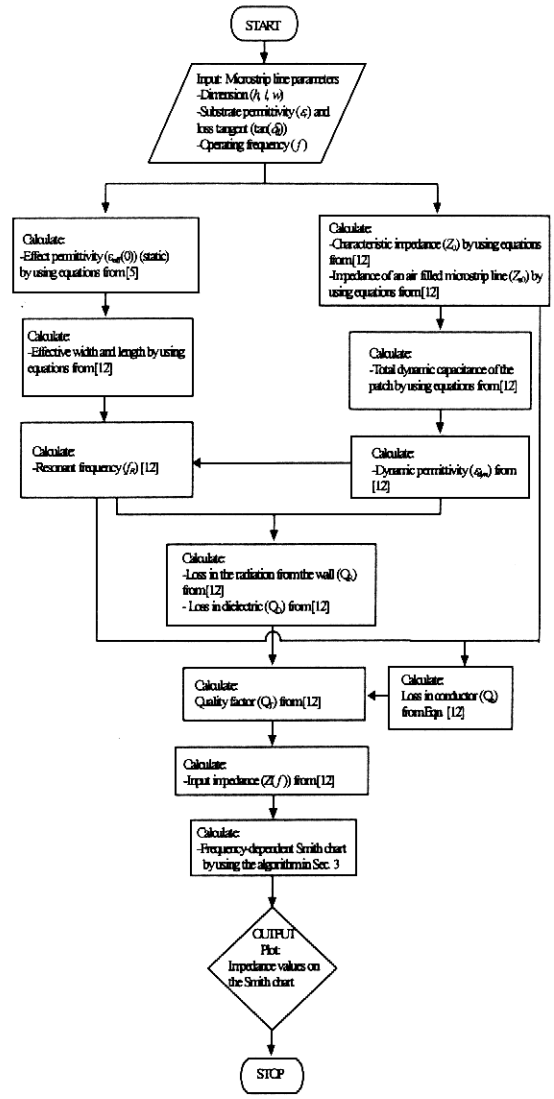

Fig. 8 Flowchart of input impedance calculation by using the proposed model

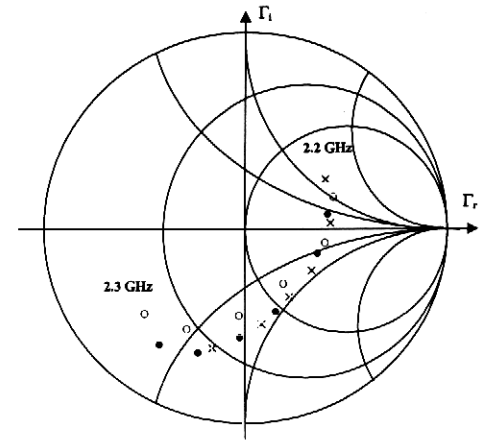

Fig. 9 Input impedance of coax-fed microstrip patch antenna $\varepsilon_r = 2.5$; Loss tangent = 0.002; h = 1.524 mm; d_o = 1.27 mm; $Z_0 = 50$ Ω; w = 68.58 mm; l = 41.40 mm; $x_o = 0.0$; mode (m = 0, n = 1)
O Measured [14] × Calculated [12] • Proposed model

The present effort addresses the design of an antenna system for wireless communication applications, which operates in the 2.45 GHz (ISM) band. The input impedance of the antenna is based upon the proposed model in the Section 4. The design of the matching section for the antenna is followed the procedure in [15].

For the present design, the rectangular microstrip antenna has a substrate with dielectric constant (ε_r) of 2.5 and the antenna is a direct-feed type. The size of the patch is 4.10 cm (w) × 4.14 cm (l) ($w = 0.3350\lambda$; $l = 0.3382\lambda$ at $f =$ 2.45 GHz) and a thickness of $h = 0.1524$ cm ($h = 0.0125\lambda$ at f = 2.45 GHz). Fig. 10 shows the input impedances calculated as per the present model and that by the Abboud's model [12] for the patch operating at 2.45 GHz. The design of the matching section for the antenna will be the next step and is discussed in the following sections.

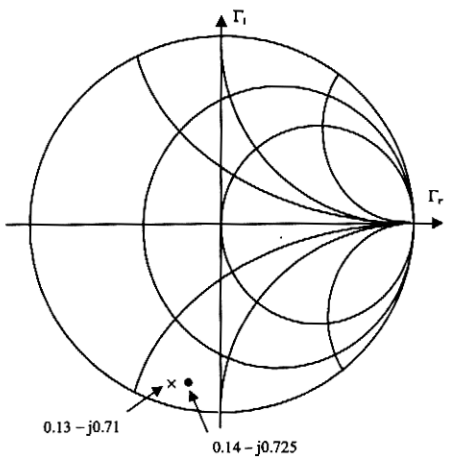

Fig. 10 The input impedance for a patch operating at 2.45 GHz
• Proposed model
× Calculate [12]

The quarter-wave transformer is a simple structure compatible for matching a real load impedance to a transmission line. An additional feature of the quarter-wave transformer is that it can be extended to multisection designs for broader bandwidths. A complex load impedance such as that indicated in Fig. 10 can always be transformed to a real part by using an appropriate length of transmission line between the load and the transformer as illustrated in Fig. 11. For the example under discussion, the line-length required to transform the complex impedance to the real values are 1.236 cm (0.101λ at $f =$ 2.45 GHz) and 1.102 cm (0.09λ at f = 2.45 GHz) for the proposed model and the Abboud's model, respectively.

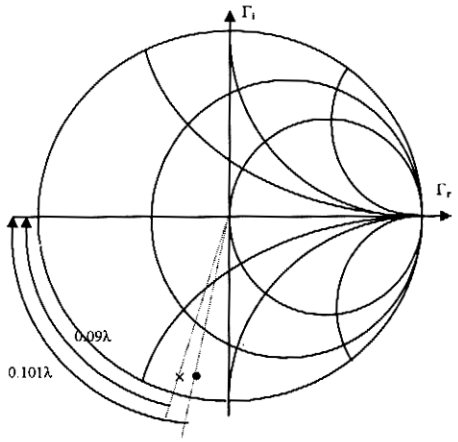

Fig. 11 Moving complex load impedance to a real impedance
• Proposed model
× Calculate [12]

The broadband design can be achieved by using a set of cascaded quarter-wave transformer sections. Assuming, that two or more quarter-wave sections are connected in cascade to transform R_R to R_{in} (Fig. 12), the problem is then to determine R'_o, R''_o, R'''_o, namely, the characteristic impedances of these sections. A number of approaches have been proposed in the literature for this purpose. For example, Everitt [15] has suggested that the use of common logarithms of the impedance ratios at the junctions in the system with the coefficients of the binomial expansion $(a+b)^n$, as indicated below:

No. of λ/4 sections, n	*Logarithm of impedance ratio*
2	1 2 1
3	1 3 3 1
4	1 4 6 4 1

For the present application, consider the design of a two-quarter-wave-section system. Reading from left to right in the inset of Fig. 12, the impedance ratios at the junctions are R_R/R'_o, R'_o/R''_o, and R''_o/R_o. Since the number of sections, n, is equal to 2,

$$\log\left(\frac{R'_o}{R''_o}\right) = 2\log\left(\frac{R''_o}{R_o}\right) = 2\log\left(\frac{R_R}{R_o}\right) \tag{31}$$

That is, from left to right, the logarithms of the impedance ratios follow the rule 1 2 1 in accordance with the above table. Then, taking antilogarithms,

$$\frac{R'_o}{R''_o} = \left(\frac{R''_o}{R_o}\right)^2 = \left(\frac{R_R}{R'_o}\right)^2 \tag{32}$$

Solving for R'_o and R''_o in terms of R_o and R_R,

$$R'_o = \frac{R_o R_R}{R''_o} \quad \text{or} \quad R'_o = \sqrt[4]{R_R^3 R_o} \tag{33}$$

$$R''_o = \frac{R_o R_R}{R'_o} \tag{34}$$

The impedance at the junction of the two quarter-wave sections is

$$R_j = \sqrt{R_R R_o} \tag{35}$$

This transformation will now be used to design a double-section system for an over-all transformation ratio of $R_R : R_o$.

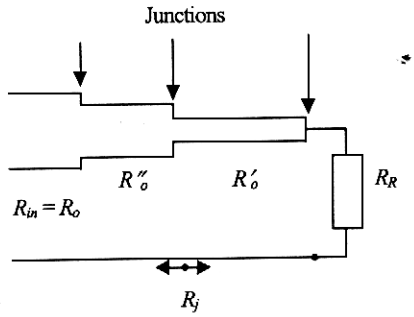

Fig. 12 Two cascaded quarter-wave transformers terminated in a constant resistive load

Consider the right-hand section, and normalized R_R with respect to R'_o:

$$r'_r = \frac{R_R}{R'_o} \tag{36a}$$

By Eqn. (35) the normalized input impedance should be

$$r'_j = \frac{R_j}{R'_o} \tag{36b}$$

Following the method of the last section, enter r'_r value on the Smith chart diagram, and rotate on a circle of constant S' the appropriate fraction of a wavelength at each frequency. The values of z'_j are tabulated in Table 1.

Now, Z_j is the termination for the left-hand quarter-wave transformer in Fig. 12. To handle this section on the Smith-diagram, all quantities should be normalized with respect to R''_o. The double prime will indicate these quantities; thus,

$$z''_j = \frac{Z_j}{R''_o} = \frac{Z_j}{R'_o}\frac{R'_o}{R''_o} = \frac{R'_o}{R''_o} z'_j \tag{37}$$

Since z''_j at each frequency and rotating toward the generator on a circle of constant S'' the appropriate distance indicated in the table. Z_{in} is determined by,

$$z_{in} = \frac{Z_{in}}{R_o} = \frac{Z_{in}}{R''_o}\frac{R''_o}{R_o} = \frac{R''_o}{R_o} z''_{in} \tag{38}$$

Table 1 Calculation of z_{in} for a quarter-wave transformer (Proposed model)

$f_o = 2.45$ GHz, $r'_r = 0.61$, $r'_j = 1.64$, $r''_j = 0.37\, r'_j$

f/f_o	l/λ	z'_j	z''_j	z''_{in}	z_{in} proposed model
1.5	0.375	0.88 – j 0.46	0.33– j 0.17	0.91 – j 1.16	0.54 + j 0.66
1.4	0.350	1.03 – j 0.51	0.38 – j 0.19	1.47 – j 1.15	0.88 + j 0.67
1.3	0.325	1.20 – j 0.51	0.44 – j 0.19	1.94 – j 0.70	1.14 + j 0.39
1.2	0.300	1.42 – j 0.44	0.53 – j 0.16	1.90 – j 0.20	1.12 + j 0.12
1.1	0.275	1.60 – j 0.25	0.59 – j 0.09	1.70 – j 0.02	1.02 + j 0.02
1.0	0.250	1.68	0.62	1.64	0.95
0.9	0.225	1.60 + j 0.25	0.59 + j 0.09	1.70 + j 0.02	1.00+ j 0.01
0.8	0.200	1.42 + j0.44	0.53 + j 0.16	1.90 + j 0.20	1.10 + j 0.10
0.7	0.175	1.20 + j 0.51	0.44 + j 0.19	1.94 + j 0.70	1.15 + j 0.37
0.6	0.150	1.03 + j 0.51	0.38 + j 0.19	1.47 + j 1.15	0.87 + j 0.66
0.5	0.125	0.88 + j 0.46	0.33 + j 0.17	0.91 + j 1.16	0.54 + j 0.68

From Fig. 13, it can be seen that, when the maximum standing wave ratio is stipulated as 2, the allowable bandwidth of the proposed model shows a greater value than that of the Abboud's model [12], to an extent of about 10%. A possible explanation is that $\Delta f / f$ (bandwidth) is directly proportional to the loss of the system [16]. Therefore, when the frequency-dependent characteristic impedance is taken into the calculation, it is reflected in an increase of bandwidth calculated (using proposed model). The structure and dimension of the designed antenna is obtained in Fig. 14 and Table 2.

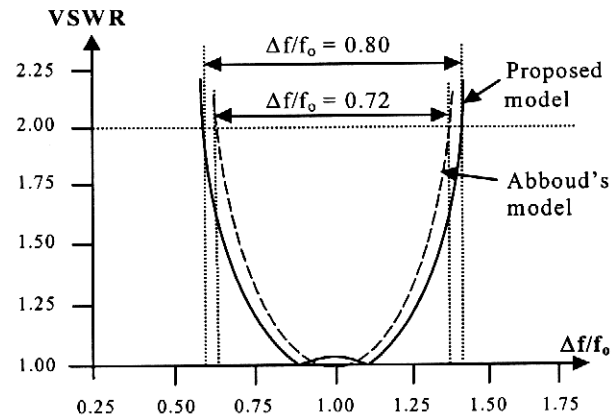

Fig. 13 Comparison bandwidth between Abboud's model and proposed model with VSWR ≤ 2.0

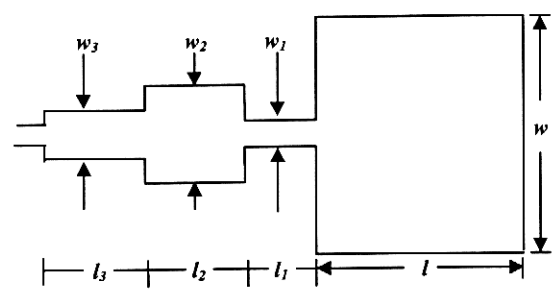

Fig. 14 Antenna structure and double-wave-transformer

Table 2 Comparison between Abboud's model and proposed model (f_o = 2.45 GHz)

Model	Abboud's model	Proposed model	Δ(% difference)
w_1	0.435 cm ($0.0355\lambda_o$)	0.435 cm ($0.0355\lambda_o$)	0
w_2	2.950 cm ($0.2410\lambda_o$)	2.785 cm ($0.2275\lambda_o$)	5.59
w_3	0.880 cm ($0.0719\lambda_o$)	0.884 cm ($0.0722\lambda_o$)	0.45
l_1	1.102 cm ($0.0900\lambda_o$)	1.236 cm ($0.1010\lambda_o$)	10.84
l_2	3.060 cm ($0.2500\lambda_o$)	3.060 cm ($0.2500\lambda_o$)	0
l_3	3.060 cm ($0.2500\lambda_o$)	3.060 cm ($0.2500\lambda_o$)	0
Bandwidth (GHz)	1.764	1.960	10.00

6. CONCLUSIONS

The use of frequency-dependent Smith-chart deduced via microstrip-based Cole-Cole diagram representation is proved to be a method representing the frequency-dependent characteristics of microstrip lines. The present study demonstrates the feasibility of a cohesive presentation of the dispersion (lossy and lossless) characteristics of a microstrip structure via Cole-Cole diagram format, which is compatible for CAD efforts.

In summary, the technique described in this chapter offers a strategy of portraying the frequency-dependent characteristics of microstrip structures via a modified Smith-chart representation. Further, as far as the author knows of, this is the first attempt in depicting the dispersion characteristics of a microstrip line via Cole-Cole diagram format.

REFERENCES

[1] M. Kobayashi, "A dispersion formula satisfying recent requirement in microstrip CAD," vol. 36, pp. 1246-1250, Aug. 1988.

[2] P. Pramanick and P. Bhartia, "An accurate description of dispersion in microstrip," Microwave J., vol. 26, no. 12, pp. 89-92, Dec. 1983.

[3] E. hammerstad and O. Jensen, "Accurate models for microstrip computer aided design," IEEE MTT-S Int. Microwave Symp. Dig., New York, NY, June 1980, pp. 407-409.

[4] E. Yamashita, K. Atsuki, and T. Veda, "An accurate dispersion formula of microstrip line for computer-aided design of microwave integrated circuits," IEEE Trans. Microwave Theory Tech., vol. MTT-27, pp. 1036-1038, Dec. 1979.

[5] M. Kirschning and R. H. Jansen, "Accurate model for effective dielectric constant with validity up to millimeter-wave frequency," Electron. Lett., vol. 18, pp. 272-273, Jan. 1982.

[6] A. K. Verma and R. Kumar, "New empirical unified dispersion model for shielded-, suspended-, and composite-substrate microstrip line for microwave and mm-wave applications," IEEE Trans. Microwave Theory Tech., vol. MTT-46, pp. 1187-1192, Aug. 1998.

[7] A. K. Verma and R. Kumar, "A new dispersion model for microstrip line," IEEE Trans. Microwave Theory Tech., vol. MTT-46, pp. 1183-1187, Aug. 1998.

[8] E. Riande and E. Saiz, Dipole Moments and Birefringence of Polymers, New Jersey: Prentice Hall, 1992.

[9] R. Coelho, Physics of dielectrics for engineer. Netherlands: Elsevier, 1979.

[10] C. S. Walker, Capacitance, Inductance and Crosstalk Analysis. Norwood, MA: Artech House, 1990.

[11] J. C. Freeman, Fundamentals of Microwave Transmission Lines, John Wiley & Sons, Inc., NewYork, 1995.

[12] F. Abboud, J. P. Damiano, and A. Papiernik, "Simple model for the input impedance of coax-fed rectangular microstrip patch antenna for CAD", IEE Proc. H, Microwaves, Antenna & Progag., vol. 135, pp. 323-326, 1988.

[13] M. D. Deshpande and M. C. Bailey, "Input impedance of microstrip antenna," IEEE Trans. Antennas Propagat., vol. 30, pp. 645-650, Dec. 1982.

[14] K. R. Carver and E. L. Coffey, "Theoretical investigation of the microstrip antenna," Technical Report 00929. Physical Science Laboratory, New Mexico State University, Las Cruces (New Mexico),

[15] Everitt and Anner, Communication Engineering, 3rd edition , Mcgraw-Hill, 1956.

[16] S. Drabowitch, A. Papiernik, H. Griffiths, and J. Encinas, Printed antenna, Ch. 6 in Modern Antennas, Chapman & Hall, Cambridge, 1998.